

Supporting Information

Z-scheme g-C₃N₄/TiO₂ Heterojunction for a High Energy Density Photo-Assisted Li-O₂ Battery

Zhichao Xue¹, Yingyi Ru², Qiang Li², Xiaolong Liang², Ying Ma⁴, Hong Sun^{2*}, Ying Lv^{3*}

¹Department of Science, Shenyang Jianzhu University, Shenyang 110168, Liaoning, China

²School of Mechanical Engineering, Shenyang Jianzhu University, Shenyang 110168, Liaoning, China

³State Key Laboratory of Luminescence and Applications, Changchun Institute of Optics, Fine Mechanics and Physics, Chinese Academy of Sciences, Changchun, 130033, China

⁴School of Materials Science and Engineering, Shenyang Jianzhu University, Shenyang 110168, Liaoning, China

*** Corresponding author:**

E-mail addresses: lvying@ciomp.ac.cn (Y. Lv), sunhongwxh@sina.com (H. Sun)

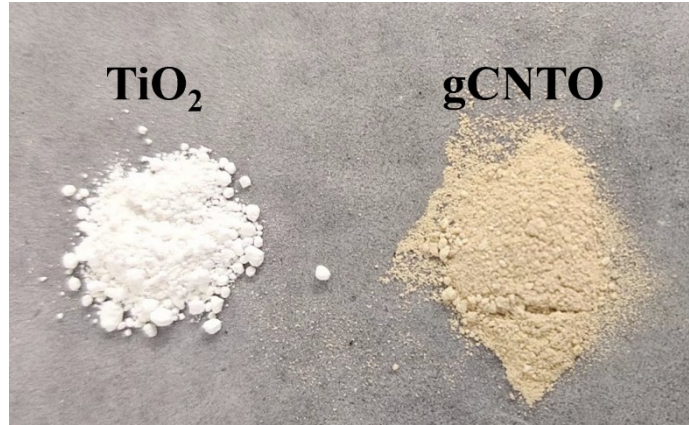


Figure S1 Digital photos of TiO_2 and $\text{g-C}_3\text{N}_4/\text{TiO}_2$

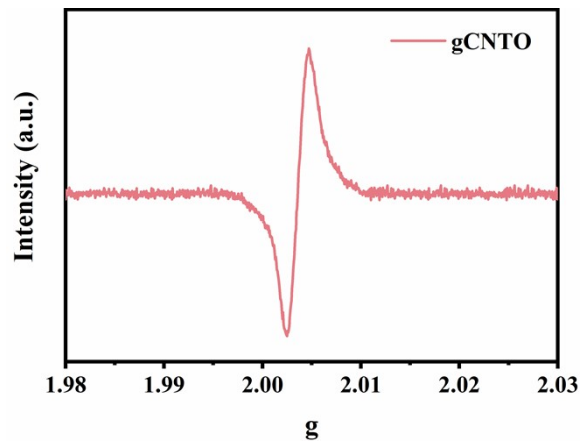


Figure S2. EPR image of $\text{g-C}_3\text{N}_4/\text{TiO}_2$.

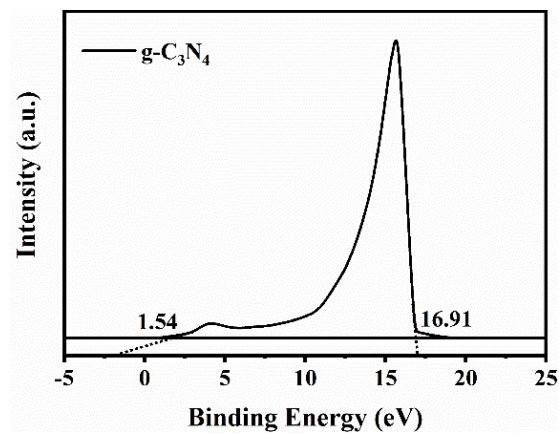


Figure S3. UPS image of $\text{g-C}_3\text{N}_4$.

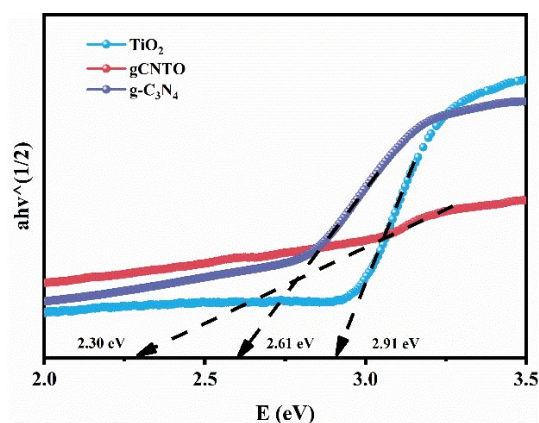


Figure S4. The Tauc plots converted from the UV-Vis spectrum show that the E_g of TiO_2 , gCNTO, g- C_3N_4 are 2.30 eV, 2.61 eV, 2.91 eV. Respectively

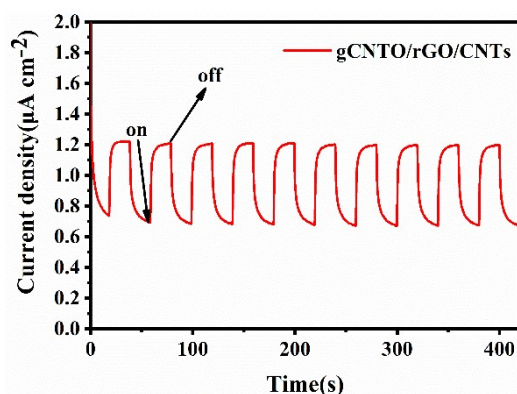


Figure S5. i-t curve of gCNTO/rGO/CNTs

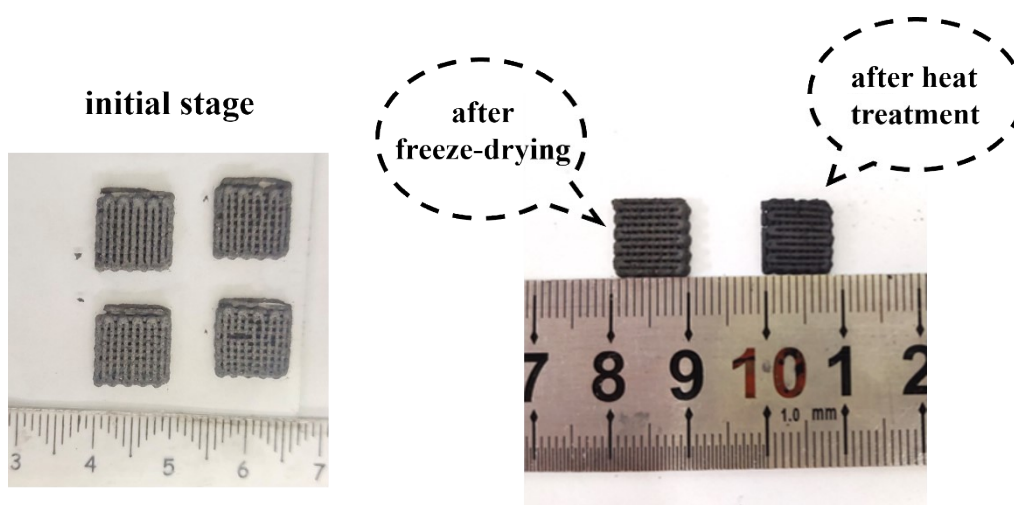


Figure S6. The 3D-printed cathode was printed into a gris structure with a

diameter of 10 mm. The structure of the printed cathode was well maintained after both freeze-drying at $-24\text{ }^{\circ}\text{C}$ and heat treatment at $500\text{ }^{\circ}\text{C}$. (After annealing, the mass of the gCNTO/rGO/CNTs electrode was $13 \pm 3\text{ mg cm}^{-2}$, and the gCNTO of the mass loading is approximately $4.78 \pm 0.7\text{ mg cm}^{-2}$ for each gCNTO/rGO/CNTs photocathode. The gCNTO/rGO/CNTs photocathode is a self-supporting cathode without current collector.)

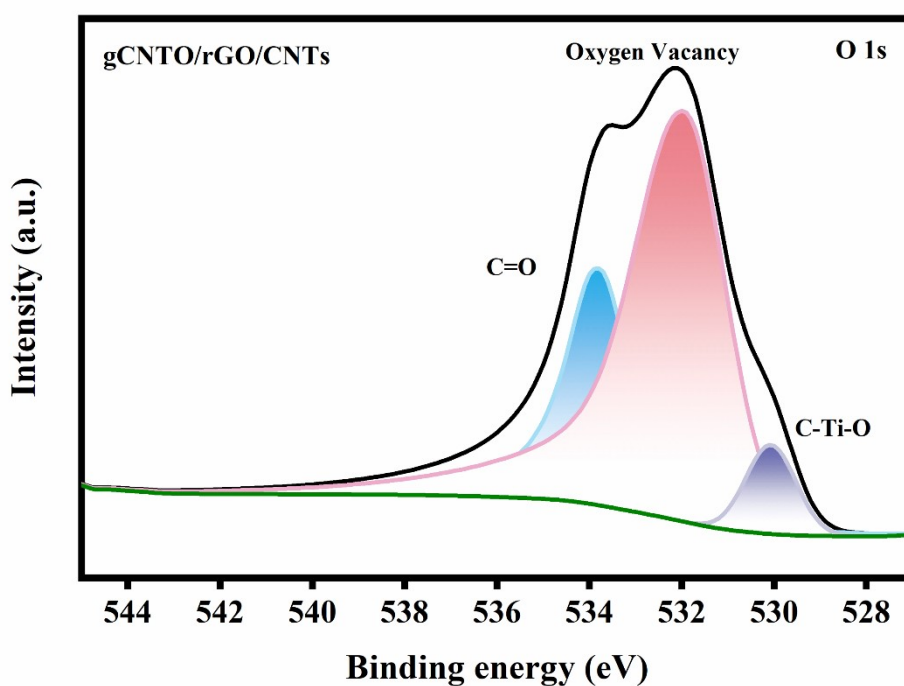


Figure S7. The XPS patterns of O 1s for gCNTO/rGO/CNTs are composed of three peaks. The peaks correspond to C=O, Oxygen vacancy, and C-O-Ti bonds, respectively.

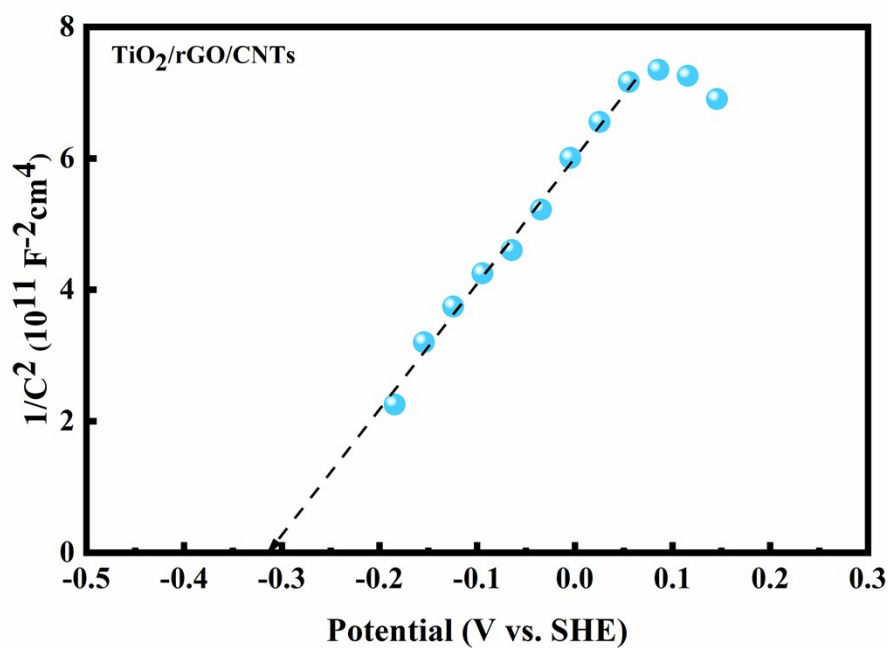


Figure S8. M-S plots of $\text{TiO}_2/\text{rGO}/\text{CNTs}$ show the flatband potential is -0.31 (vs. SHE) and has a positive slope.

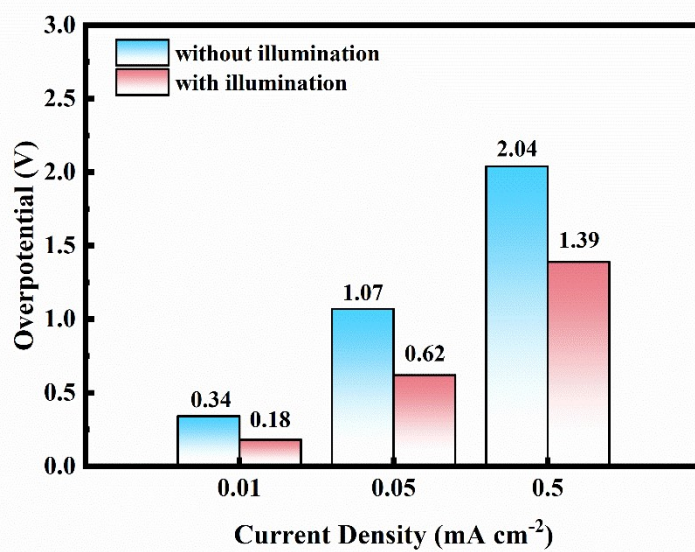


Figure S9. Discharge and charge overpotential of Li-O₂ batteries with gCNTO/rGO/CNTs cathodes under light and dark conditions.

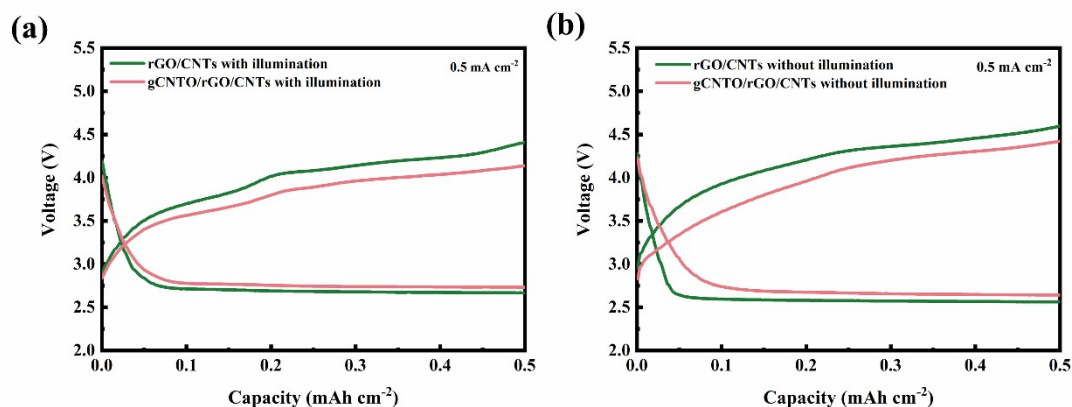


Figure S10. (a-b) Charge and discharge profiles of gCNTO/rGO/CNTs and rGO/CNTs at 0.5 mA cm⁻² with and without illumination.

The overpotential of the rGO/CNTs photocathode with illumination is 1.75 V (gCNTO/rGO/CNTs photocathode is 1.4 V), while the overpotential without illumination is 2.04 V (gCNTO/rGO/CNTs photocathode is 1.77 V). It can be clearly observed that the overpotential of the gCNTO/rGO/CNTs photocathode with illumination is significantly smaller than that of the rGO/CNTs photocathode under the same conditions.

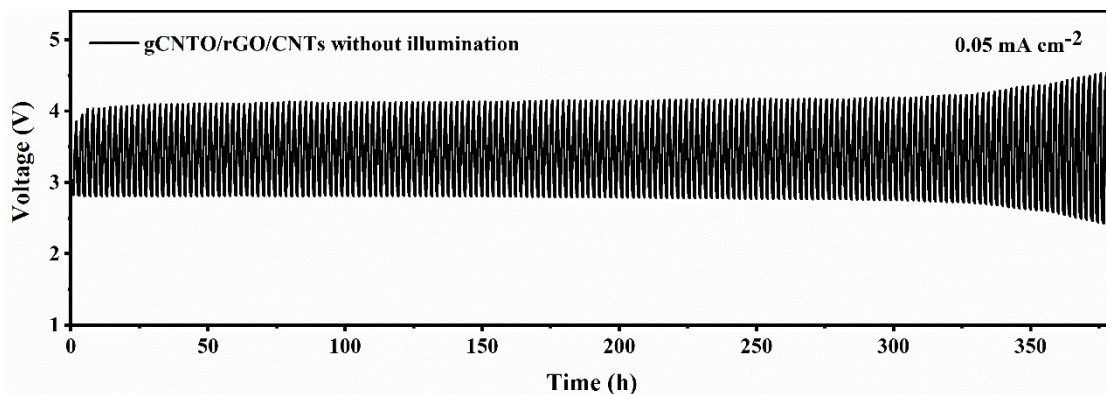


Figure S11. The cycle performance of the gCNTO/rGO/CNTs photocathode without illumination at 0.05 mA cm^{-2}

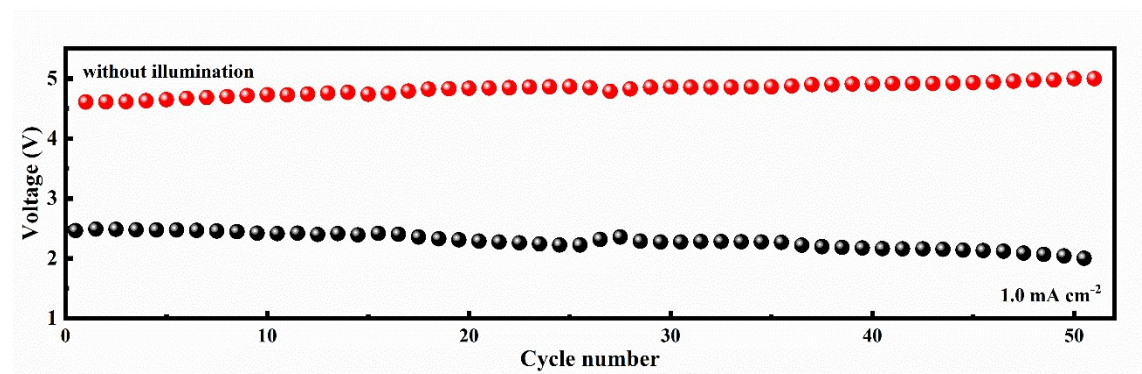
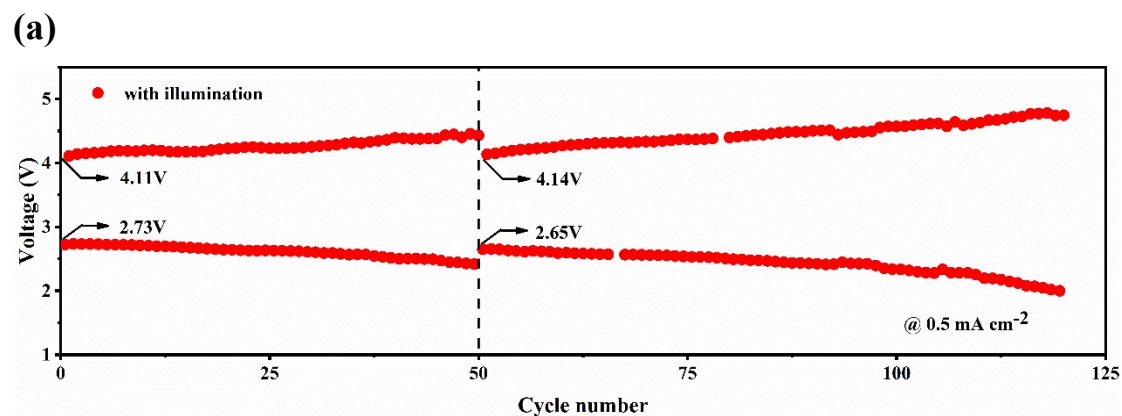


Figure S12. The gCNTO/rGO/CNTs cathode can cycle in the dark for 50 cycle number (100 hours) at a current density of 1.0 mA cm^{-2} .



(b)

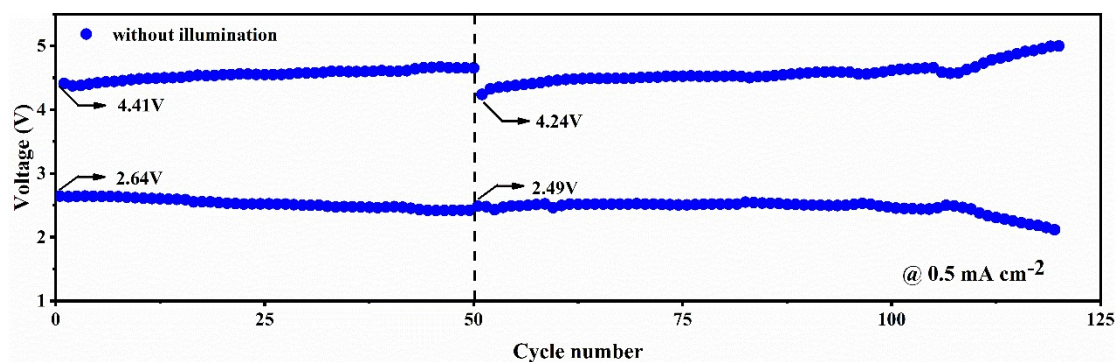


Figure S13. (a-b) The 50th cycle number of the gCNTO/rGO/CNTs cathode with and without illumination at the current density of 0.5 mA cm⁻². Then, replacing the lithium foil in the battery that gCNTO/rGO/CNTs cathode discharge voltage decay to 2.0 V.

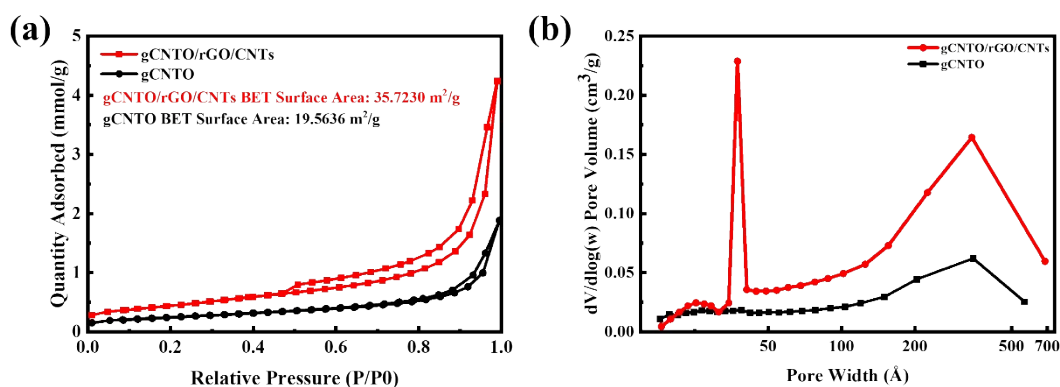


Figure S14. (a-b) The N₂ adsorption and desorption isotherms and pore size distributions of the gCNTO and gCNTO/rGO/CNTs cathode.

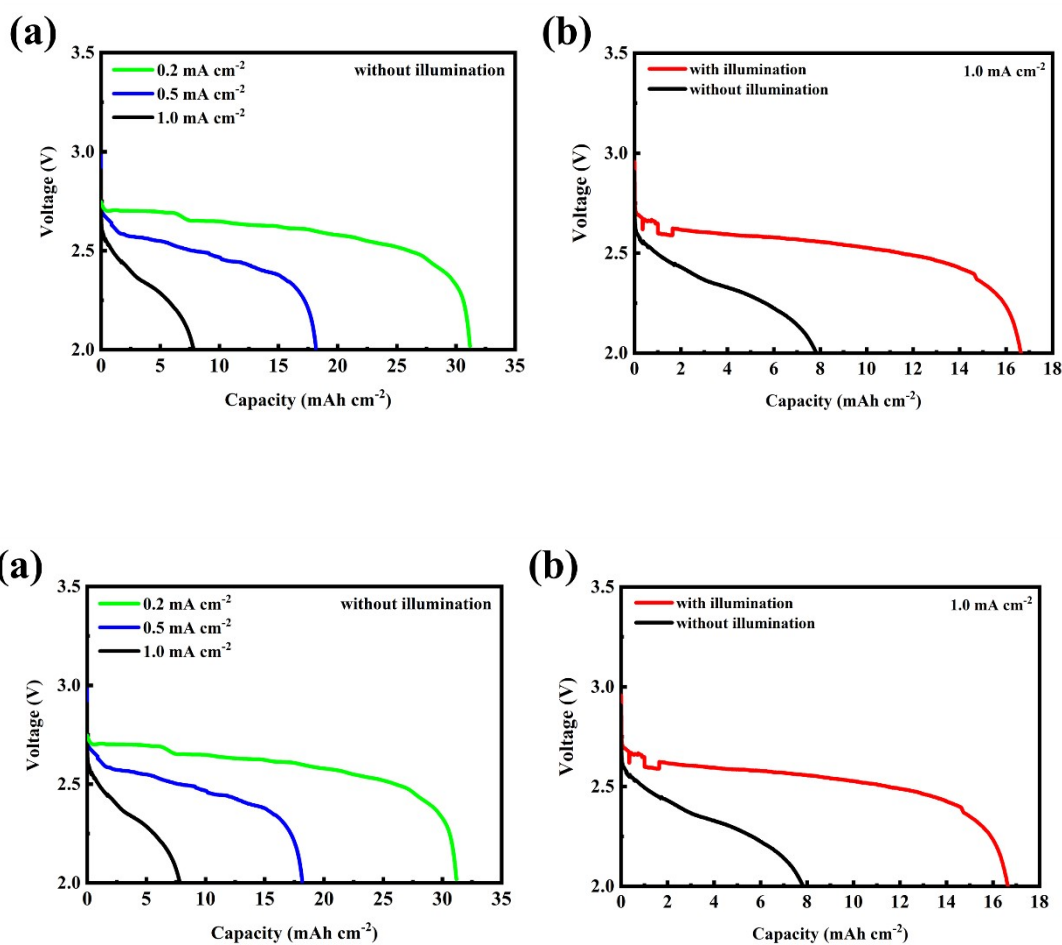


Figure S15. (a-b) Discharge capacities of gCNTO/rGO/CNTs cathode at different current densities. Li-O₂ battery of gCNTO/rGO/CNTs cathode under dark conditions demonstrated ultrahigh discharge capacities of 31.19 mAh cm⁻² at 0.2 mA cm⁻², 18.16 mAh cm⁻² at 0.5 mA cm⁻² and 7.83 mAh cm⁻² at 1.0 mA cm⁻². In contrast, the discharge capacity of 16.64 mAh cm⁻² at 1.0 mA cm⁻² under light conditions.

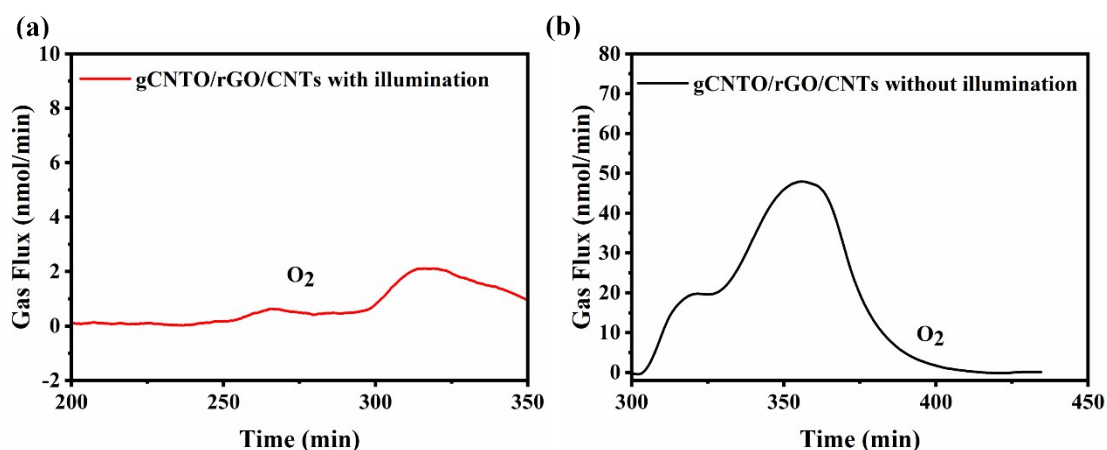


Figure S16 The DEMS charging test results of (a) gCNTO/rGO/CNTs with illumination (b) gCNTO/rGO/CNTs without illumination

Table S1

Discharge capacity of Li-O₂ battery in recent years

Cathode	Current Density	Discharge Capacity	Load	Ref
gCNTO/rGO/CNTs	0.5 mA cm⁻²_{light} (105 mA g ⁻¹)	29.73 mAh cm⁻² (6220 mAh g ⁻¹)	4.78 ± 0.7 mg cm⁻² (gCNTO)	This work
	0.5 mA cm⁻²_{dark} (105 mA g ⁻¹)	18.16 mAh cm⁻² (3799 mAh g ⁻¹)		
	1.0 mA cm⁻²_{light} (209 mA g ⁻¹)	16.64 mAh cm⁻² (3481 mAh g ⁻¹)		
N ₀ -wdC-900	0.05 mA cm ⁻²	9.44 mAh cm ⁻²	unknown	[1]
Co@NC/PPC-800	0.2 mA cm ⁻²	10.0 mAh cm ⁻²	0.5 ± 0.1 mg	[2]

			cm ⁻² (catalyst)	
Ru-NPC@CBC	0.2 mA cm ⁻²	4.93 mAh cm ⁻² (12890 mAh g ⁻¹)	unknown	[3]
Air-breathable-textile-based cathode	0.1 mA cm ⁻²	8.6 mAh cm ⁻²	unknown	[4]
MoS ₂ /MoN@CC	0.1 mA cm ⁻²	9.04 mAh cm ⁻²	unknown	[5]
CVO@CNT	0.1 mA cm ⁻²	6.14 mAh cm ⁻²	unknown	[6]
CoPt/AFC	0.05 mA cm ⁻² (100mA g ⁻¹)	8.25 mAh cm ⁻² (16505 mAh g ⁻¹)	unknown	[7]
LKAC	0.2 mA cm ⁻²	1.6 mAh cm ⁻²	unknown	[8]
3D-hierarchical Co/CoO/C	0.1 mA cm ⁻²	4.8 mAh cm ⁻²	unknown	[9]
WNF-0.45	0.2 mA cm ⁻²	23.11 mAh cm ⁻²	unknown	[10]
G6-Co-T	0.05 mA cm ⁻²	2.19 mAh cm ⁻² (5635 mAh g ⁻¹)	1.3 mg cm ⁻² (cathode)	[11]
RuO ₂ -Co ₃ O ₄ @CC	0.3 mA cm ⁻²	2.91 mAh cm ⁻²	2.5 mg cm ⁻² (cathode)	[12]
SnO ₂ @C45	0.5 mA cm ⁻²	6.5 mAh cm ⁻²	unknown	[13]
iPPM iPPM@Li	0.05 mA cm ⁻²	28.14 mAh cm ⁻²	unknown	[14]
O-CNP@NiFe(OH) _x	0.25 mA cm ⁻²	27.5 mAh cm ⁻²	unknown	[15]
PdSnCo/NG	0.3 mA cm ⁻²	6.75 mAh cm ⁻² (6750mAh g ⁻¹)	1.0 ± 0.1 mg cm ⁻² (catalyst)	[16]

Biphasic N-doping cobalt@graphene	0.1 mA cm ⁻²	6.0 mAh cm ⁻²	1.0 mg cm ⁻² (cathode)	[17]
--------------------------------------	-------------------------	--------------------------	--------------------------------------	------

Equation S1

The specific energy of the photo-assisted Li-O₂ battery were calculated based on the following equation,

$$\text{Specific energy (} \frac{Wh}{g \text{ cell}} \text{)} = \text{Specific capacity (} \frac{Ah}{g \text{ cell}} \text{)} \times \text{potential (V)}$$

Our calculations indicate a specific capacity of 515.12 Wh kg⁻¹_{cell} of in the light at an average discharge potential of 2.60 V with a total mass of 0.15 g including the gCNTO/rGO/CNTs cathode, electrolyte, Fiberglass, and Li metal anode. Similarly, the average discharge potential in the dark state is 2.47 V. An energy density of 298.72 Wh kg⁻¹_{cell} is obtained from the above equation.

Reference

- [1] S. Jing, Z. Gai, M. Li, S. Tang, S. Ji, H. Liang, F. Chen, S. Yin, P. Tsiakaras, Enhanced Electrochemical Performance Of A Li-O₂ Battery Using Co And N Co-Doped Biochar Cathode Prepared In Molten Salt Medium, *Electrochimica Acta* 410(1) (2022) 140002. <https://doi.org/https://doi.org/10.1016/j.electacta.2022.140002>.
- [2] H.G. Liang, L.H. Jia, F. Chen, Three-Dimensional Self-Standing Co@NC Octahedron/Biochar Cathode For Non-Aqueous Li-O₂ Batteries: Efficient Catalysis For Reversible Formation And Decomposition Of LiOH, *Journal of Materials Science* 55(18) (2020) 7792-7804. <https://doi.org/10.1007/s10853-020-04574-x>.
- [3] M.L. Wang, Y. Yao, F.Y. Yang, Z.W. Tang, J.J. Ren, C.Z. Zhang, F. Wu, X.K. Wang, Double Spatial Confinement On Ruthenium Nanoparticles Inside Carbon Frameworks As Durable Catalysts For A Quasi-Solid-State Li-O₂ Battery, *CARBON ENERGY* 5(8) (2023) e334.
- ..
- [4] S.M. Xu, Y.G. Yao, Y.Y. Guo, X.Q. Zeng, S.D. Lacey, H.Y. Song, C.J. Chen, Y.J. Li, J.Q. Dai, Y.B. Wang, Y.A. Chen, B.Y. Liu, K. Fu, K. Amine, J. Lu, L.B. Hu, Textile Inspired Lithium-Oxygen Battery Cathode With Decoupled Oxygen And Electrolyte Pathways, *ADVANCED MATERIALS* 30(4) (2018) 1704907.

<https://doi.org/10.1002/adma.201704907>.

[5] Y.T. Gu, Y. Ma, L. Wei, Y.B. Lian, Y. He, Y.H. Su, X.J. Li, Y. Peng, Z. Deng, Conformal Lithium Peroxide Growth Kinetically Driven By MoS₂/MoN Heterostructures Towards High-Performance Li-O₂ Batteries, BATTERIES & SUPERCAPS 5(9) (2022) e202200222. <https://doi.org/10.1002/batt.202200222>.

[6] D. Li, X. Lang, Y. Guo, Y. Wang, Y. Wang, H. Shi, S. Wu, W. Wang, Q.-H. Yang, A Photo-Assisted Electrocatalyst Coupled With Superoxide Suppression For High Performance Li-O₂ Batteries, Nano Energy 85 (2021) 105966. <https://doi.org/https://doi.org/10.1016/j.nanoen.2021.105966>.

[7] H. Xia, Q. Xie, Y. Tian, Q. Chen, M. Wen, J. Zhang, Y. Wang, Y. Tang, S. Zhang, High-Efficient CoPt/activated Functional Carbon Catalyst For Li-O₂ Batteries, Nano Energy 84 (2021) 105877. <https://doi.org/https://doi.org/10.1016/j.nanoen.2021.105877>.

[8] G.Z. Zhang, Y. Yao, T. Zhao, M.L. Wang, R.J. Chen, From Black Liquor to Green Energy Resource: Positive Electrode Materials for Li-O₂ Battery With High Capacity And Long Cycle Life, ACS APPLIED MATERIALS & INTERFACES 12(14) (2020) 16521-16530. <https://doi.org/10.1021/acsami.0c01520>.

[9] C. Hua, Z. Qian, M. Chen, C. Du, P. Zuo, X. Cheng, Y. Ma, G. Yin, 3D Hierarchical Co/CoO/C Nanocomposites With Mesoporo

us Microsheets Grown On Nickel Foam As Cathodes For Li-O₂ Batteries, Journal of Alloys and Compounds 749(15) (2018) 378-384. <https://doi.org/https://doi.org/10.1016/j.jallcom.2018.03.297>.

[10] L. Wei, Y. Su, Y. Ma, Y. Gu, Y. Qin, X. Wu, Y. He, X. Li, Y. Peng, Z. Deng, Photoluminescent WSe₂ Nanofibers As Freestanding Cathode For Solar-Assisted Li-O₂ Battery With Ultrahigh Capacity And Transparent Casing, Chemical Engineering Journal 448(15) (2022) 137591. <https://doi.org/https://doi.org/10.1016/j.cej.2022.137591>.

[11] W.H. Wang, A.Y. Tesio, M. Olivares-Marín, P.G. Romero, D. Tonti, Facile Preparation Of Glycine-Based Mesoporous Graphitic Carbons With Embedded Cobalt Nanoparticles, JOURNAL OF MATERIALS SCIENCE 57(28) (2022) 13403-13413. <https://doi.org/10.1007/s10853-022-07421-3>.

[12] X. Peng, M. Li, L. Huang, Q. Chen, W. Fang, Y. Hou, Y. Zhu, J. Ye, L. Liu, Y. Wu, RuO₂-Incorporated Co₃O₄ Nanoneedles Grown On Carbon Cloth As Binder-Free Integrated Cathodes For Tuning Favorable Li₂O₂ Formation, ACS Applied Materials & Interfaces 15(1) (2023) 1401-1409. <https://doi.org/10.1021/acsami.2c19399>.

[13] J. Amici, P. Marquez, A. Mangini, C. Torchio, D. Dessantis, D. Versaci, C. Francia, M.J. Aguirre, S. Bodoardo, Sustainable, Economic, And Simple Preparation Of An Efficient Catalyst for Li-O₂ Batteries, Journal Of Power Sources 546(30) (2022) 231942. <https://doi.org/https://doi.org/10.1016/j.jpowsour.2022.231942>.

- [14] Y. He, L.Y. Ding, J. Cheng, S.W. Mei, X.L. Xie, Z.Y. Zheng, W.Y. Pan, Y.Z. Qin, F.D. Huang, Y. Peng, Z. Deng, A "Trinity" Design Of Li-O₂ Battery Engaging The Slow-Release Capsule Of Redox Mediators, *ADVANCED MATERIALS* 35(49) (2023) 2308134. <https://doi.org/10.1002/adma.202308134>.
- [15] B. Zhao, Z. Ye, X. Kong, L. Han, Z. Xia, K. Chen, Q. Wang, M. Li, Y. Shang, A. Cao, Orthogonal-Channel, Low-Tortuosity Carbon Nanotube Platforms For High-Performance Li-O₂ Batteries, *ACS Nano* 17(18) (2023) 18382-18391. <https://doi.org/10.1021/acsnano.3c05782>.
- [16] X. Ren, B. Liao, Y. Li, P. Zhang, L. Deng, Y. Gao, Facile Synthesis Of PdSnCo/nitrogen-Doped Reduced Graphene As A Highly Active Catalyst For Lithium-Air Batteries, *Electrochimica Acta* 228(20) (2017) 36-44. <https://doi.org/https://doi.org/10.1016/j.electacta.2017.01.032>.
- [17] G.Q. Tan, L.N. Chong, R. Amine, J. Lu, C. Liu, Y.F. Yuan, J.G. Wen, K. He, X.X. Bi, Y.Y. Guo, H.H. Wang, R. Shahbazian-Yassar, S. Al Hallaj, D.J. Miller, D.J. Liu, K. Amine, Toward Highly Efficient Electrocatalyst For Li-O₂ Batteries Using Biphasic N-Doping Cobalt@Graphene Multiple-Capsule Heterostructures, *NANO LETTERS* 17(5) (2017) 2959-2966. <https://doi.org/10.1021/acs.nanolett.7b00207>.